Mineralogical Magazine, February 2004, Vol. 68(1), pp. 1–14

Optimization of some key geothermobarometers for pelitic metamorphic rocks

M. J. HOLDAWAY*,†

Department of Geological Sciences, Southern Methodist University, Dallas, Texas, 75275, USA

ABSTRACT

I will consider mainly geothermobarometry in medium-grade pelitic rocks, including the garnet-biotite (GB) geothermometer, the Grossular-Al silicate-plagioclase (GASP) geobarometer, and the muscovite-almandine-biotite-sillimanite (MABS) geobarometer. For GB (Holdaway, 2000) experimental data and estimated biotite ΔW_{Ti} were used to optimize two exchange parameters and four biotite Margules parameters. Using stepwise linear regression, experimental *vs*. calculated T were constrained to lie on a line with slope of one and intercept of zero, maximizing r^2. The best model involves experiments by Ferry and Spear (1978) and Perchuk and Lavrent'eva (1983), suggesting minimal ^{vi}Al in the Ferry and Spear product biotite. For GASP (Holdaway, 2001), end-member experimental data do not adequately constrain the equilibrium. I used the GB model above, and allowed the end-member curve to rotate about the best-constrained part of the GASP end-member data. The end-member curve was further constrained with the kyanite-sillimanite (K-S) boundary using published chemical data on 76 pelitic schist samples from 11 localities, rejecting Low-Grs and low-An samples. The Fuhrman and Lindsley (1988) plagioclase model gives the best results. For MABS, work in progress involves 61 samples from the 11 localities which have muscovite analyses. Biotite Margules parameters were based on the GB model and McMullin *et al*. (1991). The MABS end-member curve was calibrated by comparison of P values determined using trial MABS data and GASP results. The P values for the 61 samples agree well with the K-S boundary, and sillimanite-bearing rocks of west-central Maine all fall in the sillimanite field. Preliminary biotite values are: $G_{Ann} = -5149198 - 412.05\ T$, $W_{AlFe} = -14023 + 28.14\ T$, $W_{AlMg} = -259582 + 308.44\ T$, $W_{TiFe} = 124842 - 98.67\ T$, $W_{TiMg} = -186148 + 271.72\ T$. For geobarometry, the Berman (1988, revised 1992) database was used with adjustable H and S of grossular for GASP and H and S of annite for MABS. The accuracy of currently available databases, activity models and mole fraction models is not adequate for good geothermobarometry, without further refinement. Adjustable parameters tend to compensate for error in activity models, mole fraction models and databases.

KEYWORDS: geothermobarometry, pelitic rocks, garnet, mica, sillimanite, staurolite, metamorphism, Maine, USA.

Introduction

I thank the Mineralogical Society very much for inviting me to deliver the Hallimond Lecture. It is an honour for which I feel unworthy, but I am delighted to be here.

I will discuss mainly recent work that I have done, but some of the work goes back about two decades. My work over the years has benefited from the contributions of various students and colleagues, including former students Barb Dutrow, Robert Dickerson and James Novak and colleagues Biswajit Mukhopadhyay, Charles Guidotti, Darby Dyar and Frank Hawthorne. My research has been supported by the National

* E-mail: holdaway@mail.smu.edu
*Present address: 855 Elliott St., Longmont, CO 80501, USA
† Hallimond Lecture, 2002
DOI: 10.1180/0026461046810167

Science Foundation and Southern Methodist University.

I will be considering five subjects that relate to each other in various ways. (1) I will begin with a brief discussion of metamorphism in west-central Maine, my work on which has benefited greatly from collaboration with Charles Guidotti, Barb Dutrow and Darby Dyar. (2) I will briefly examine our contributions to the chemistry and crystal chemistry of staurolite. (3) Then I will summarize our work on the garnet-biotite geothermometer. (4) Following this, I discuss my work on the GASP geobarometer. (5) Finally, I will give a brief description of work in progress on the MABS geobarometer. I hope to communicate two main themes: (1) some possible ways to deal with the problem of calibration of geothermobarometers, and (2) some important aspects of the use of these and other geothermobarometers. I emphasize that no study represents 'the answer' regarding a particular method; each successive study hopefully represents further improvement in calibration as new data on both natural and experimental systems become available. It is my opinion that the best conditions for calibration and measurement of T and P are in medium-grade (amphibolite-facies) metamorphism. This is because low-grade rocks do not always fully equilibrate and high-grade rocks commonly continue to equilibrate on the retrograde part of the P-T cycle. It may then be possible, with caution, to extrapolate some of these approaches into low- and high-grade conditions.

Metamorphism in Maine

Four lobes of metamorphic activity are seen in west-central Maine, located in the northeast corner of the United States (Holdaway *et al*., 1982, 1988; Novak and Holdaway, 1981; Dickerson and Holdaway, 1989). The first event in the region (M1) was a broad chlorite-zone metamorphism which probably occurred shortly before 400 Ma and may be synchronous with much of the folding and thrusting in the region. Events which followed M1 were more thermal in nature. M2 (~400 Ma) produced staurolite-andalusite followed by sillimanite at highest grades close to plutons. M2 developed in the northern part of the area. Specifically, it is associated with northern plutons, the broad area north and west of Farmington and near Augusta, Maine. The next younger M3 has retrograded or truncated and prograded M2 zones so that most M2 rocks are significantly changed. In many such rocks the only remnant of M2 is psuedomorphs after andalusite and/or staurolite. M3 (~385 Ma) is the major event shown by the four lobes of activity (Fig. 1 of Holdaway *et al*., 1988), and involves the sequence staurolite, staurolite-sillimanite, sillimanite-muscovite at highest grades, but neither andalusite nor kyanite. Hercynian metamorphism (~325 Ma) involves the highest grades of sillimanite-muscovite and sillimanite-K-feldspar-muscovite rocks inside the sillimanite-K-feldspar isograd, near the large Sebago batholith at the southern end of the area. South of and underneath the batholith, kyanite-staurolite rocks prevail locally.

The metamorphism is largely post-kinematic in nature, indications of strain during any of the latter three events (M2, M3, and Hercynian) are rare. Major folding and thrusting in the region predates these events. In each case the metamorphism shows a spatial relationship to the mid-level plutons in the area. Tight re-entrant angles between lobes of plutonism suggest localized heat sources. In general, there is a broad increase in P both from north to south and with progressively younger events. The wide metamorphic zones relate partly to the depth of intrusion but mainly to the gentle dips of sill-like plutonic bodies. The Hercynian sillimanite-K-feldspar isograd is 20 km or more horizontally from the apparent heat source, but geophysical studies show the igneous rocks at shallow depths. In addition, this Hercynian metamorphic event shows a plateau effect with roughly constant grade throughout, and muscovite disappears completely in only a few specimens. In many respects, the Maine metamorphism is ideally suited for calibration and testing of geothermobarometers.

The staurolite enigma

As a result of working in Maine, I became interested in staurolite (Holdaway *et al*., 1986*a*,*b*, 1991, 1993; Dutrow *et al*., 1986; Dutrow and Holdaway, 1989; Dyar *et al*., 1991; Holdaway and Mukhopadhyay, 1995). I want to review briefly what we have done with this enigmatic mineral. With the help of Barb Dutrow, Frank Hawthorne and Darby Dyar, we have made some progress in demystifying staurolite. First, we found that the H content is variable and is involved in a complex vacancy-vacancy substitution with Fe, Mg, Mn, Zn and Li. In working with the ion probe to try to

measure H, we discovered that staurolite always contains at least some Li, and in some rare cases up to 25% of the divalent ions are replaced by Li, an element not normally measured with the electron probe. With Frank Hawthorne's help on the structure (Hawthorne *et al*., 1993) we have fine-tuned the crystal chemistry. We have worked out *P-T* stability relations for Fe staurolite which take into account the variable H. Finally we have estimated thermodynamic data for 2-H and 6-H Fe staurolite. Assignment of ions to sites in staurolite involves complex partitioning in multiple sites. In addition, the major Fe-Mg substitution is probably non-ideal. As a result, trying to work with this mineral is still difficult, and not much has been done to try to incorporate staurolite into geothermobarometers. Staurolite might some day serve as an H_2O barometer when it coexists with its breakdown assemblage.

The garnet-biotite geothermometer

Now we consider the GB geothermometer (Holdaway *et al*., 1997; Holdaway, 2000), designated by the equilibrium

$$\underset{\text{Pyrope}}{Mg_3Al_2Si_3O_{12}} + \underset{\text{Annite}}{KFe_3AlSi_3O_{10}(OH)_2} = \underset{\text{Almandine}}{Fe_3Al_2Si_3O_{12}} + \underset{\text{Phlogopite}}{KMg_3AlSi_3O_{10}(OH)_2}$$

One problem is that there are numerous Margules models for garnet. Three recent studies of garnet Margules models (Table 1) were published in 1996 and 1997. Figure 1 shows excess free energy of mixing for the binaries MgFe, CaFe and CaMg. Only the Mukhopadhyay *et al*. (1997) model includes errors. Note the differences in the free energy scale between plots. These models involve different methods and, to some extent, different data. There is no *a priori* reason to reject any one of these. They differ to some degree, but the similarities outweigh the differences. Two studies involve the assumption that the entropic Margules are symmetrical; the Mukhopadhyay *et al*. (1997) model allows the entropy terms to be asymmetrical as are the enthalpy terms. In my opinion, it is not necessarily best to assume symmetry, but the robust regression methods of Mukhopadhyay *et al*. (1997) may have exaggerated the asymmetry (perhaps in both S and H), so I think an average of the three models may in fact be the best presently attainable garnet model. This average model performs slightly better in geothermometry than any one individual model. Only the Ganguly *et al*. (1996) garnet model provides Margules parameters for MnMg. I found that their value, increased by 5 kJ, provides the best overall results. We will consider these four garnet models and apply them to both the garnet-biotite geothermometer and the GASP geobarometer.

Table 1 shows the garnet models and the various experimental combinations tested. The data sets are Ferry and Spear (1978, FS), Perchuk and Lavrent'eva (1983, PL) and Gessmann *et al*. (1997, GE). Ferry and Spear (1978) assumed zero ^{vi}Al in

TABLE 1. Experimental garnet-biotite sets and garnet models evaluated.

Set	Data
1	GE and FS (n = 25), GE est. of ^{vi}Al in FS biotite.
2	PL and FS (n = 47), GE est. of ^{vi}Al in FS biotite.
3	PL and FS (n = 47), GE est. of ^{vi}Al in FS biotite, garnet W_{MnMg} inc. by 5 kJ.
4	PL and FS (n = 47), 0.0 ^{vi}Al in FS biotite, garnet W_{MnMg} inc. by 5 kJ.
5	PL and FS (n = 47), 0.10 ^{vi}Al in FS biotite, garnet W_{MnMg} inc. by 5 kJ.
6	PL, FS and GE (n = 60), 0.10 ^{vi}Al in FS biotite, garnet W_{MnMg} inc. by 5 kJ.
BA	Berman and Aranovich (1996) garnet, Ganguly *et al*. (1996) W_{MnMg}.
GA	Ganguly *et al*. (1996) garnet.
MU	Mukhopadhyay *et al*. (1997) garnet, Ganguly *et al*. (1996) W_{MnMg}.
AV	Average of BA, GA and MU.

Notes: See Holdaway (2000) for additional explanation
FS – Ferry and Spear (1978) experiments for $Alm_{90}Pyr_{10}$ (n = 12).
GE – Gessmann *et al*. (1997) experiments (n = 13, 5 rejected)
PL – Perchuk and Lavrent'eva (1983) experiments (n = 35)
Mukhopadhyay *et al*. (1997) garnet volume model was used in all cases

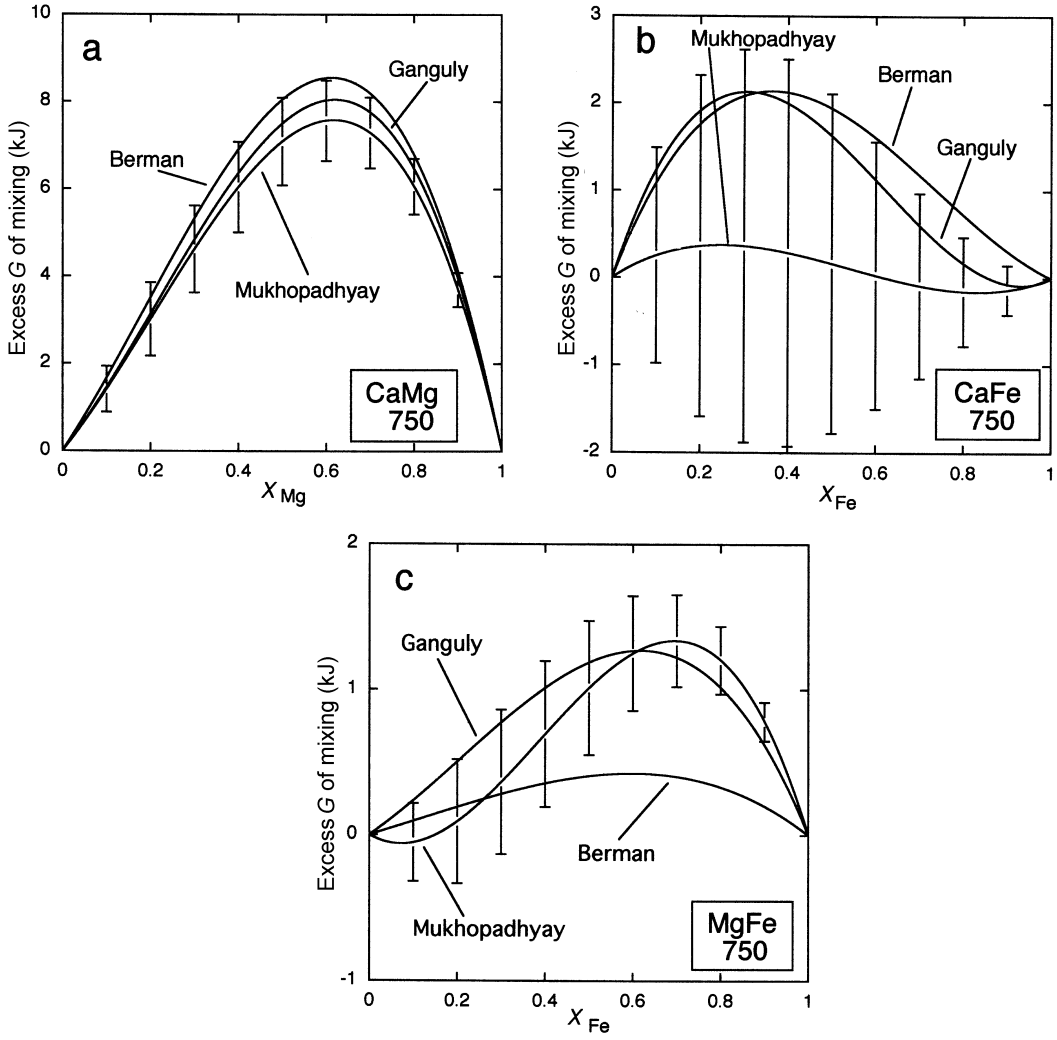

FIG. 1. Free energy of mixing calculated from the garnet binary mixing models of Berman and Aranovich (1996), Ganguly *et al*. (1996) and Mukhopadhyay *et al*. (1997), designated by first author. Box gives binary system and T (ºC). Error bars are 2σ errors of Mukhopadhyay *et al*. (1997). Reproduced from Holdaway (2000) with permission. See Holdaway (2000) for data at 500 and 1000ºC.

their product biotite, whereas Gessmann *et al.* (1997) assumed that the Ferry and Spear product biotite had substantial ^{vi}Al. Aranovich *et al*. (1988) made measurements of Al in product biotite from the PL experiments, and Perchuk and Lavrent'eva (1983) made a few measurements of Ca and Mn in product garnet and Ti in product biotite. In using their model, I optimized average Ca and Mn in product garnets and average Ti in product biotite, and the resultant values agree reasonably with the available product mineral analyses.

For the optimization process described below, I assumed Fe^{3+} values of biotite (11.6%) and garnet (3%) based on the Mössbauer analyses of Dyar (1990) and Guidotti and Dyar (1991). I used an average of the published values of ΔW_{Ti} ($W_{TiFe} - W_{TiMg}$) in biotite, including a T effect, and the volume Margules parameters of Mukhopadhyay *et al*. (1997) for garnet. This leaves six variable parameters for optimization, the H and S garnet-biotite exchange parameters, the H and S FeMg Margules parameters for biotite, and the H and S

ΔW_{Al} ($W_{AlFe} - W_{AlMg}$) Margules parameters for biotite.

For any given experimental set and garnet model, e.g. 1BA (Table 2), the optimization process involved finding the values of these six parameters that allow for calculated values of T that best fit the experimental values, as follows: (1) choose a starting set of the six parameters. (2) Calculate the T values for the various experimental data using equations 1 and 2 of Holdaway (2000) and the Margules formulations of Mukhopadhyay *et al*. (1993). (3) Regress the calculated T values against the experimental T values. (4) Adjust the six parameters and repeat the regression until the regression line reaches a slope of one and an intercept of zero. (5) Continue the regressions stepwise (maintaining a slope of one and intercept of zero) until a maximum value of r^2 is reached for that model. This procedure gives the maximum value of r^2 to within 0.001.

TABLE 2. Statistical data for various garnet biotite models.

Model	r^2	σ (º)	σ_i/σ (%)
1BA	0.892	26.7	46.4
1GA	0.895	26.3	48.8
1MU	0.896	26.1	48.5
2BA	0.956	23.3	43.3
2GA	0.944	26.4	47.5
2MU	0.943	26.5	47.5
3BA	0.955	23.5	42.2
3GA	0.943	26.5	45.8
3MU	0.943	26.6	45.8
4BA	0.980	15.4	41.0
4GA	0.980	15.3	43.9
4MU	0.982	14.5	43.6
5BA	0.9802	15.33	40.96
5GA	0.9805	15.21	43.95
5MU	0.9825	14.40	42.27
5AV	0.9815	14.81	42.23
6BA	0.9419	24.95	42.39
6GA	0.9394	25.52	44.36
6MU	0.9437	24.54	43.53
6AV	0.9425	24.81	42.99

Notes: Models given in Table 1. See text for details
r^2 = experimental goodness of fit
σ = standard deviation of $T_{calc} - T_{exp}$
σ_i/σ = Maine M3 and Hercynian metamorphic data, weighted average σ of six zones and assemblages over total σ, a measure of degree of separation of the zones in T

Table 2 summarizes the results in terms of statistical parameters. The values of r^2 and σ for the experimental data are negatively correlated, as expected for regressions with slope of one and intercept of zero. The last column relates to an independent test of each maximum-r^2 data set used to calculate T values for the M3 and Hercynian events in Maine (98 specimens). The parameter σ_i/σ provides a measure of how well the six zones and assemblages separate from each other in T. Minimum values indicate the least overlap and are therefore considered best. Through successive experimental models 1 to 5, the maximum r^2 increases and σ and σ_i/σ decrease (Table 2). The model 5AV provides the best overall combination of maximum r^2 and minimum σ and σ_i/σ. Figure 2 shows calculated *vs*. experimental T values for the previously most recent model of Gessmann *et al*. (1997) and for my results. For Gessmann's geothermometer, the regression line is not constrained to have a slope of one and an intercept of zero. It has lower r^2 and higher σ than my results. The parameters for my best result (5AV) are (in Joules per mole) $\Delta G_{ex} = 40198 - 7.80\ T$, biotite $W_{FeMg} = 22998 - 17.40\ T$, biotite $\Delta W_{Al} = 245559 - 280.31\ T$. The equations for calculating T are equations 1 and 2 of Holdaway (2000), and the equations for calculating the activity of pyrope and almandine in garnet and annite and phlogopite in biotite as a function of T and P are given by Mukhopadhyay *et al*. (1993). The M3 staurolite zone in Maine has an average T of 571±12ºC, and the sillimanite-muscovite zone (without staurolite) has an average T of 619±11ºC. Error under optimum conditions is estimated to be ±15º relative and ±25º absolute. In analysing minerals for garnet-biotite T determinations, the analysed biotite grains should be near but not in contact with the garnet. Normally the outer rim or the peak-T portion of the garnet should be analysed. The same part of the P-T cycle must be represented by all the minerals analysed. Finally, when using the work of any author on geothermometry, the activity and mole fraction models of the author must be used in order to minimize error. See Holdaway (2000) for additional details.

The GASP Geobarometer

The GASP geobarometer (Holdaway, 2001) involves the equilibrium

$$\underset{\text{Grossular}}{Ca_3Al_2Si_3O_{12}} + \underset{\text{Al silicate}}{2Al_2SiO_5} + \underset{\text{Quartz}}{SiO_2} = \underset{\text{Plagioclase}}{3CaAl_2Si_2O_8}$$

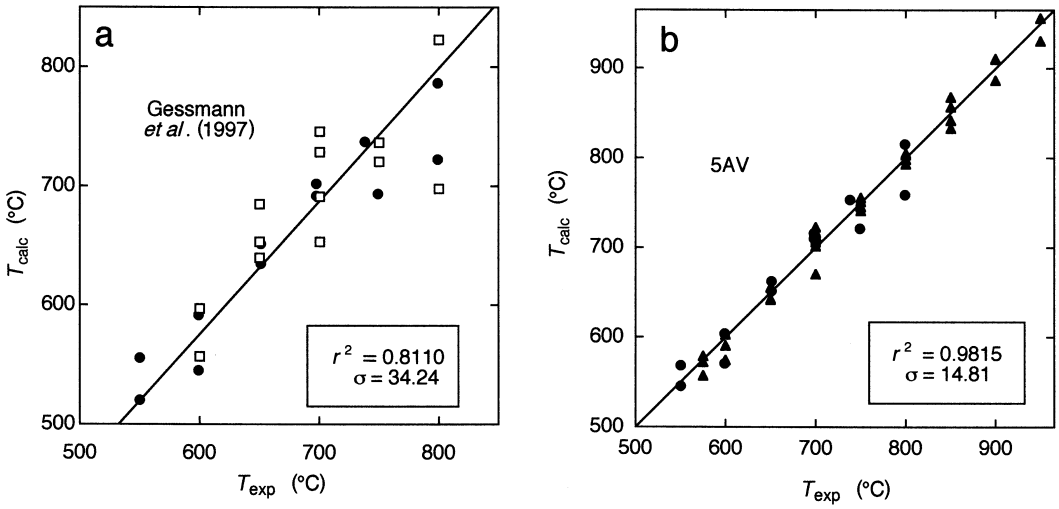

FIG. 2. Plots of calculated *vs*. experimental garnet-biotite *T* for (*a*) the model of Gessmann *et al*. (1997) and (*b*) the results of Holdaway (2000), model 5AV. Solid triangles = PL data, solid dots = FS data, open squares = GE data. Only the experiments used to create the calibration model are shown. Box gives values of r^2 and σ. Reproduced from Holdaway (2000) with permission.

I begin with an assertion which I believe to be true: it is an unfortunate fact of life that many (or most) geobarometers for low- and medium-grade metamorphism must be calibrated, at least in part, using secondary methods. Direct experimental data are at present not precise enough at geological values of *T* and *P* to be useful. The only geobarometer which is experimentally calibrated in the range of medium grade with any reasonable degree of accuracy is the K-S equilibrium. Secondary methods are necessary to calibrate any other geobarometer.

The three kinds of experimental data needed to calibrate a geobarometer are (1) an end-member calibration, (2) a way to determine *T* and estimate its error, and (3) activity models for any minerals which are not pure phases, in this case garnet and plagioclase. Figure 3*a* illustrates the end-member constraints. Note that I am plotting *T* against Δ*P* from the least-squares line through the experimental data for the GASP end-member *P-T* diagram (*P* (kbar) = 0.022 *T* − 6.2). In this way the data can be shown in more detail. All the reversal data from five consistent studies are shown here, each point extended 1σ away from equilibrium. The least-squares line plots at zero Δ*P*. On this plot are shown the steepest and flattest possible lines through the reversal data. Ideally, the end-member calibration should correspond to the least-squares line. We shall see that in fact it comes closer to the steepest possible line through the data. When these steepest and flattest lines are extended down to geological *T* values, there is a great deal of latitude. Below, I will choose the intersection of these two lines as the best-constrained part of the end-member system.

I have chosen data from a single sillimanite-bearing specimen which formed at about 575ºC, 5.25 kbar to illustrate the problem of the amount of latitude provided by the existing experimental constraints (Table 3). The four *T* columns illustrate the ±25ºC error on 575ºC. The first two columns represent the Fuhrman and Lindsley (1988) plagioclase activity model and the last two the Elkins and Grove (1990) plagioclase model. The first three rows represent the flattest possible end-member curve and the last three the steepest, and the garnet models are abbreviated as in Table 1. To summarize, the maximum possible *P* range for this one specimen is 8 kbar, one kbar each due to garnet, plagioclase and *T* error, and about 5 kbar due to end-member calibration. In addition, most of the determinations fall in the kyanite field.

From this observation, we can conclude that (1) additional constraints are needed, (2) the least-squares GASP end-member curve is too flat or too high in *P*, (3) some adjustable parameter is needed not only to adjust the end-member curve but to compensate for differences in garnet and plagioclase models. Possible approaches include (1) add

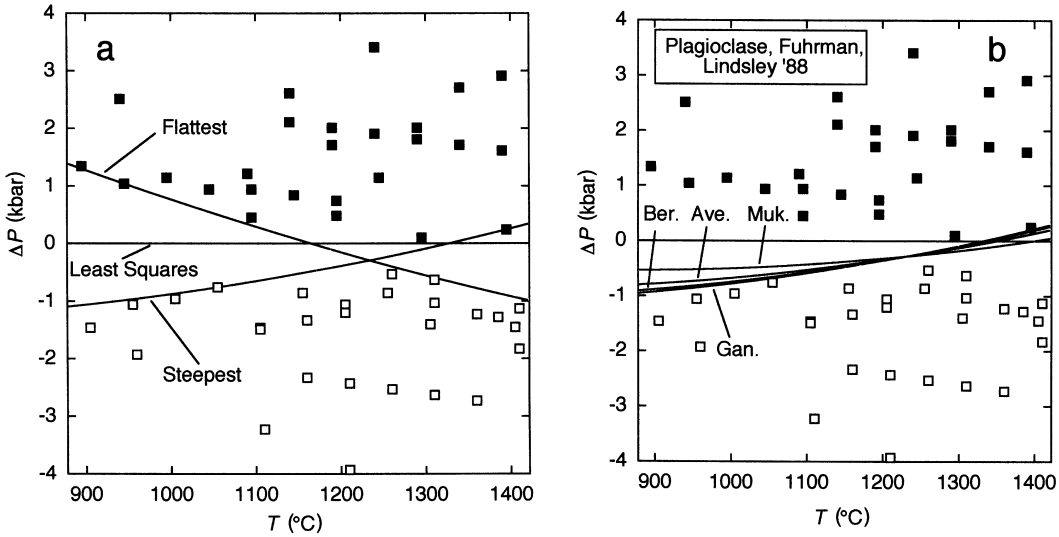

FIG. 3. Plots of ΔP *vs*. T of end-member data for the GASP reaction, designed for maximum amplification. ΔP is the P difference between the McKenna and Hodges (1988) least-squares line, P (kbar) = 0.022 T (K) − 6.2, and experimental or calculated P data. Squares are GASP experimental data extended 1σ away from the equilibrium curve: closed = grossular + kyanite + quartz stable, open = anorthite stable. Except for the horizontal least-squares line, lines are calculated from the Berman (1988, revised 1992) database with H_{Grs} and S_{Grs} allowed to vary to fit the situation as described in text. (*a*) Flattest and steepest possible curves consistent with extended reversals, (*b*) GASP end-member curves based on Holdaway (2001) results using the Fuhrman and Lindsley (1988) plagioclase activity model. Garnet activity models are Ber. = Berman and Aranovich (1996), Gan. = Ganguly *et al*. (1996), Muk. = Mukhopadhyay *et al*. (1997). Reproduced from Holdaway (2001) with permission.

additional constraints to the end-member curve as are provided in thermodynamic databases or (2) use some other equilibrium from natural samples to constrain the end-member curve.

Let us consider the pros and cons of databases for use in thermobarometry. On the one hand, (1) they allow use of several equilibria to constrain the P and T, and (2) they are consistent. On the other hand, (1) consistency does not equate to accuracy, (2) systematic errors in thermodynamic data may cause discrepancies between various compositions or between various P-T

TABLE 3. GASP P range for sample 2-13 due to range in end-member calibration, plagioclase activity model, garnet activity model, and T error of ±25ºC.

Plagioclase model	Fuhrman and Lindsley (1988)		Elkins and Grove (1990)	
T (ºC)	550	600	550	600
MU-F	9.1	9.7	10.1	10.5
BA-F	10.1	10.6	11.1	11.4
GA-F	10.1	10.6	11.1	11.4
MU-S	3.5	4.5	4.5	5.3
BA-S	4.5	5.4	5.5	6.2
GA-S	4.5	5.4	5.5	6.2

Notes: F – flattest possible slope of end-member curve, S – steepest possible slope of end-member curve (Fig. 3*a*). Garnet models given in Table 1. Sample is a representative sillimanite-bearing rock from Azure Lake, British Columbia, Canada (Pigage, 1982). See text and Holdaway (2001) for details.

TABLE 4. Localities, references and mineral composition ranges of samples used for GASP calibration and verification.

Locality	Reference	% Grs range	% An range
Hunt Valley Mall, MD, USA	Lang (1991)	5–7	20–29
Mt. Moosilauke, NH, USA	Hodges and Spear (1982)	4–6	24–27
Azure Lake, BC, Canada	Pigage (1982)	4–10	20–39
Augusta, Maine, USA	Ferry (1980)	3–7	22–47
West-Central ME, USA	Holdaway *et al*. (1988)	3–7	18–53
Quabbin Reservoir, MA, USA	Tracy (1975)	4–5	27–40
Grampian Highlands, Scotland	McLellan (1985)	5–13	18–32
Snow Peak, ID, USA	Lang and Rice (1985*a,b*)	5–11	17–33
West-Central NH, USA	Spear *et al*. (1995)	3–8	21–39
Yale, BC, Canada	Pigage (1976)	7–14	26–34
Penfold Cr., BC, Canada	Fletcher and Greenwood (1979)	4–9	26–36
Lepontine Alps, Switzerland	Engi *et al*. (1995); Todd and Engi (1997)	3–23	17–74

conditions, and (3) each new constraint to the end-member curve adds another source of error. In addition, the thermodynamic database must be made consistent with the activity models to be used, and the activity models themselves contain systematic errors.

Here is the approach I used in calibrating the eight possible models (2 plagioclase times 4 garnet models, including the average garnet model). I wrote three programs to calculate the *T*, *P* and the *P-T* intersection. I used the garnet-biotite geothermometer discussed above (Holdaway, 2000). I used the Berman (1988, updated 1992) Ge0calc database with adjustable parameters, standard enthalpy and entropy of grossular. The *P* was calculated using equation 2 of Holdaway (2001). I constrained the end-member curve to pass through the intersection of the steepest and flattest end-member curve discussed previously (Fig. 3*a*). I employed the garnet, biotite and plagioclase chemical data from 11 localities (76 samples) using the K-S boundary to further constrain the end-member curve by adjusting H and S of grossular in the database to produce the best overall fit of the K-S curve from calculated *P-T* points. Three samples which misfit the K-S curve by >1 kbar by all models were rejected as disequilibrium. The results were verified using a separate data set from the Alps (59 samples).

I used the peak-*T* assemblage. Samples with Grs (^{viii}Ca in garnet) <3% (4% for older analyses), An <17% (22% for older analyses) were rejected because both analytical error and activity model error become exaggerated at high dilution. I used the rim compositions of garnet and plagioclase unless they were retrograde, and in that case I used the peak-*T* compositions. I used the highest-*T* Al silicate present in more than trace amounts. The 11 localities and the Lepontine Alps and their references and composition ranges are given in Table 4.

TABLE 5. Comparison of two previous GASP calibrations and eight present calibrations using the 11 localities of Table 4 (kJ/mole, J/ ºmole, kbar).

Model	$-H_{Grs}$	S_{Grs}	EMV	OR	MP	#Vio
HS82	6626	261	−0.58	1.16	−0.14	10
B92	6633	255	−0.43	0.84	0.16	5
MUF	6622	263	0.00	0.85	−0.06	4
BAF	6631	257	0.00	0.84	0.09	4
GAF	6633	256	0.00	0.87	−0.01	4
AVF	6629	259	0.00	0.85	0.00	4
MUE	6631	257	0.00	0.81	−0.06	4
BAE	6641	250	−0.13	0.81	0.12	4
GAE	6642	250	−0.15	0.83	−0.01	3
AVE	6638	252	−0.07	0.81	0.01	3

Notes: Models: HS82 – Hodges and Spear (1982), B92 – Berman (1988, updated, 1992), first two letters of remaining models as in Table 1, F – Fuhrman and Lindsley (1988), E – Elkins and Grove (1990).
EMV – Maximum end-member violation, e.g. Fig. 3*b*,
OR – overlap range relative to K-S line e.g. Fig. 4,
MP – midpoint of overlap range relative to K-S line,
#Vio – number in violation of K-S line >0.15 kbar.
AVF is the favoured calibration for reasons discussed in text. See Holdaway (2001) for additional details.

Table 5 illustrates standard grossular H and S data for the eight present models and two previous models (Hodges and Spear (1982), which was used as recently as 1995, and Berman (1988, updated 1992)). Figure 3*b* shows the end-member curves for the four models which involve Fuhrman and Lindsley (1988) plagioclase, which I consider to be the best (see below). Figures 4 and 5 illustrate the fit of the AVF model with the K-S boundary for the 11 localities and the Alpine samples, respectively. A substantial range of standard grossular H and S results from the various models, but at 1230ºC, the standard free energy of grossular is the same for all eight present models, as a result of the method of calibration. Table 5 also gives some points of comparison for the 10 models applied to the 76 samples from 11 localities: maximum end-member violation, overlap range on the K-S boundary, mid-point of the overlap range relative to the K-S boundary, and the number of samples that violate the K-S boundary by more than 150 bar. The eight models are slightly better than the Berman (1988, updated 1992) model and substantially better than the Hodges and Spear (1982) model. The Fuhrman and Lindsley (1988) plagioclase fits the end-member data a little better than the Elkins and Grove (1990) model.

The simple plagioclase model of Hodges and Spear (1982) fails for the Alpine samples as a result of the high range of An content (Fig. 4*a* of Holdaway, 2001). In all models, the overlap range is twice as large or more for the Alpine samples than for the 11 localities (compare Figs 4 and 5). This is due to the larger overall *P* range of the Alps, larger than for any of the other 11 localities, which probably translates to larger *P* ranges for individual samples and larger error in determining the peak-*T* conditions.

Figure 6 shows a scatter plot of the *P* difference between the two plagioclase models, using the average garnet activity, including the 11 localities and the Alps. In the common range of plagioclase composition, the two plagioclase models agree well, but at low and especially at high An content, the two disagree substantially. The high An

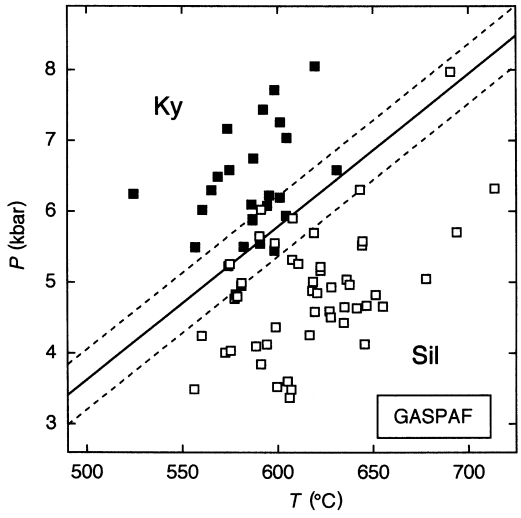

FIG. 4. Calculated *P* and *T* for 76 samples from the 11 localities given in Table 4 using GASP and GB (three samples were rejected as explained in text). Closed squares represent samples that contain kyanite as the peak-*T* mineral, and open squares samples that contain sillimanite. Solid line is K-S boundary, and dashed lines parallel to the K-S boundary delimit the field of overlap, in which either kyanite or sillimanite may be present as the peak-*T* mineral. The model shown is the preferred Fuhrman and Lindsley (1988) plagioclase with the average garnet model (AVF). Additional models are given by Holdaway (2001). Reproduced from Holdaway (2001) with permission.

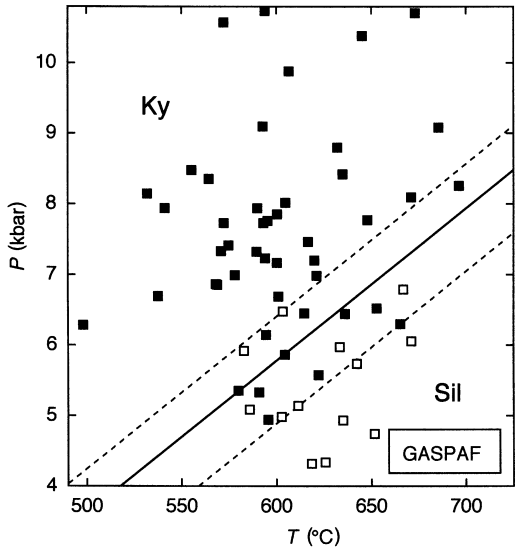

FIG. 5. Calculated *P* and *T* for 59 samples from the Lepontine Alps using GASP and GB (four samples were rejected as explained in text). Other information is as given in the caption for Fig. 4. The model shown is the preferred Fuhrman and Lindsley (1988) plagioclase with the average garnet model (AVF). Additional models are given by Holdaway (2001). Reproduced from Holdaway (2001) with permission.

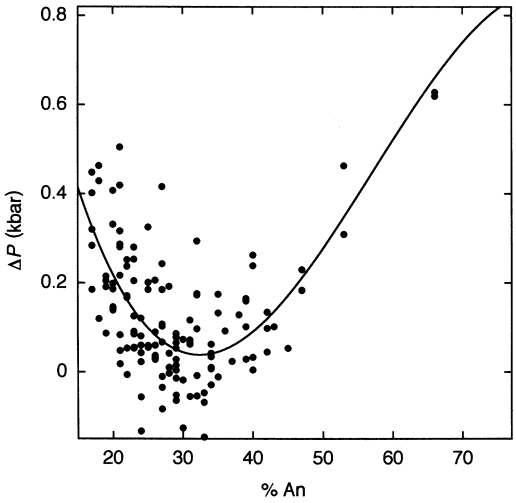

FIG. 6. Scatter plot of $P_{AVF} - P_{AVE}$ (ΔP) *vs*. %An for 76 samples from the 11 localities and 59 samples from the Lepontine Alps (Table 4). The rough agreement between the two models between An_{22} and An_{48} is the result of the method of calibration. See text for further explanation. Reproduced from Holdaway (2001) with permission.

content samples come mainly from the Alps. I will try to quantify the effect of An content on the plagioclase model. On the basis of the garnet-biotite *T* work we conclude that the average garnet model is best, and the GASP results give no further insight into this problem (Table 5, Fig. 3*b*). I want to compare the two plagioclase models which differ most at high and low An. The weighted average σ in *P* is 1.5% lower for the Elkins and Grove (1990) plagioclase model than for Fuhrman and Lindsley (1988) plagioclase, for the 11 localities. However, the average *P* shift (from end-member to actual P) is 8% lower for Elkins and Grove (1990) plagioclase. Thus the weighted average sigma should be more than 8% lower in order for the Elkins and Grove model to be better. This is a telescoping effect. For the Alps, with higher range of An %, the sigma for the two models is the same, and again, the Elkins and Grove model should be at least 8% lower in order for it to be better. Therefore the Fuhrman model (based on an Al-avoidance model) is most accurate. (This analysis is detailed in Holdaway, 2001).

There are three independent sources of error, *T* error on *P*, K-S error, and misfit error with the K-S diagram. The root-mean-square average of these gives 800 bar absolute and 600 bar relative. The largest contribution to the error is geological error which affects K-S misfit error. This is seen by the fact that the areas with the largest K-S misfit are those with the largest standard deviation in *P*, the Grampian Highlands and the Alps (Holdaway, 2001). Low An or Grs, within the stated limits, does not increase the misfit. The equation for calculating *P* is equation 2 of Holdaway (2001), the equation for calculating activity of grossular in garnet is given by Mukhopadhyay *et al*. (1993), and the preferred equation for calculating activity of anorthite in plagioclase is given by Fuhrman and Lindsley (1988).

Here are some suggestions for obtaining the best possible GASP *P* determinations: (1) reject samples with low grossular or anorthite content. (2) Especially for electron microprobes which might have spectrometer drift, analyse Fe and Mg in garnet and biotite, and Ca in garnet and plagioclase, as close as possible in time. (3) Obtain the best possible *T*. (4) Analyse two or more sets in the same thin section or outcrop in order to get some idea of the reproducibility of the results. (5) Analysed plagioclase and biotite should be spatially near the analysed garnet, but not in contact with garnet. (6) The same part of the rock's history must be represented by the part of each mineral that is analysed and by the Al silicate chosen. Much of the geological error that I experienced with the 11 localities and the Alpine samples could have been reduced or eliminated by more care in these aspects.

The MABS geobarometer

Finally, I will take a brief look at my efforts so far on the MABS (muscovite-almandine-biotite-sillimanite) geobarometer, involving the equation

$$\underset{\text{Muscovite}}{KAl_3Si_3O_{10}(OH)_2} + \underset{\text{Almandine}}{Fe_3Al_2Si_3O_{12}} = \underset{\text{Annite}}{KFe_3AlSi_3O_{10}(OH)_2} + \underset{\text{Al silicate}}{2Al_2SiO_5} + \underset{\text{Quartz}}{SiO_2}$$

Advantages of this geobarometer are that there are substantial amounts of each reaction component present in pelitic minerals, and the assemblage is very common in medium-grade pelites. The main disadvantage of MABS is the absence of any experimental calibration whatsoever. As with GASP, I began with three programs to calculate *T*, *P* and their intersection, using the Holdaway (2000) garnet-biotite geothermometer. I used the Berman (1988, updated 1992) database

with H and S of annite as adjustable parameters. The biotite TiFe and TiMg Margules parameters are based on data determined for the garnet-biotite geothermometer (Holdaway, 2000) and data from McMullin *et al*. (1991). Biotite ΔAl is based on Holdaway (2000). Using the same 11 localities (Table 4), there are 61 usable samples with complete muscovite analyses. I optimized the MABS *P* against the GASP *P*. I then verified the results against the K-S line using the 11 localities and the Maine M3 and Hercynian data set which contain sillimanite as the Al silicate.

By successive approximation, plotting P_{MABS} less P_{GASP} (ΔP) against *T*, I found the annite H and S and biotite W_{AlFe} and W_{AlMg} (consistent with the Holdaway, 2000 ΔW_{Al}) for which a regression of the data yields a horizontal line at zero ΔP (Fig. 7). Four data with ΔP >2 kbar were rejected as probable disequilibrium. Solutions for which regressions yield zero ΔP exist over a range of thermodynamic conditions. One solution, annite *G* (J/mole) = −5149198 − 412.05 *T*, W_{AlFe} = −14023 + 28.14 *T*, W_{AlMg} = −259582 + 308.44 *T*, W_{TiFe} = 124842 − 98.67 *T*, W_{TiMg} = −186148 + 271.72 *T*, provides a low standard deviation for the ΔP *vs*. *T* plot (Fig. 7), and is tentatively adopted here. The equation for calculating *P* is the same as the GASP equation (Holdaway, 2001), and activities of almandine in garnet and annite in biotite are given by Mukhopadhyay *et al*. (1993).

The resultant K-S plot for the 11 localities is given in Fig. 8. The four with kyanite which plot in the sillimanite field within about 1 kbar of the K-S line from two localities in British Columbia, Canada (Azure Lake and Penfold Creek, Table 4). For both of these localities it has been independently suggested that the muscovite is, at least in part, late, and may not have been at equilibrium with the rest of the assemblage. The remaining samples fit the K-S boundary rather well.

Figure 9 gives the conditions for Maine M3 and Hercynian metamorphism based on MABS for *P* and GB for *T*. The sillimanite-K-feldspar-muscovite samples of the Hercynian metamorphism scatter to high *P*, while the sillimanite-muscovite samples within the same sillimanite-K-feldspar isograd are more tightly bunched at the bottom of the sillimanite-K-feldspar-muscovite trend. Based on this analysis, one might conclude that the reason for partial breakdown of muscovite is reduced H_2O activity, since the two sets of data plot on the same trend. The samples for both metamorphic events plot entirely within the sillimanite field; the sillimanite-andalusite boundary is below the plot.

Table 6 lists the conditions of metamorphism for Maine as an average and two standard deviations for *T* and *P*. These data can be used to get a rough idea of the relative *P* error. For the first three zones, a significant part of the 2σ variation in *P* must be error, suggesting that the relative error is on the order of 600 bar. Absolute

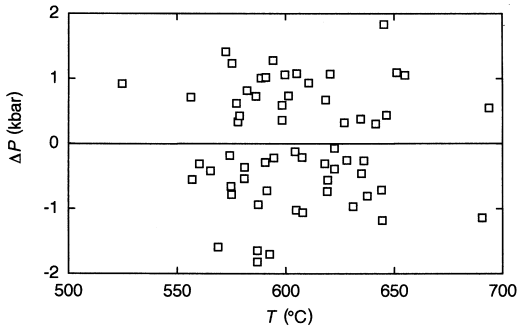

FIG. 7. Plot of P_{MABS} less P_{GASP} (ΔP) against *T* determined by GB for 61 samples from the 11 localities given in Table 4. Solid line at zero ΔP is the least-squares regression of the data. Four samples with ΔP >2 kbar were rejected as probable disequilibrium.

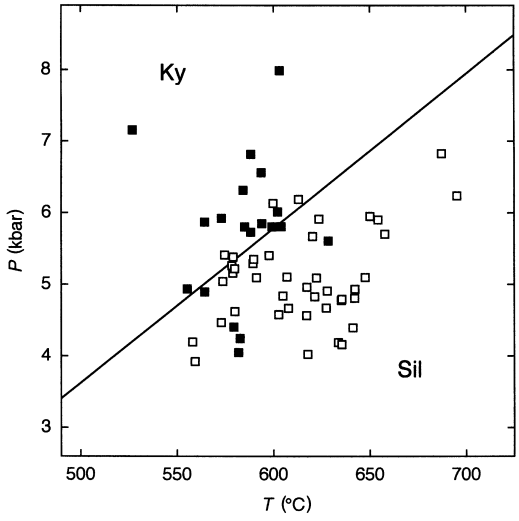

FIG. 8. Calculated *P* and *T* for 61 samples from the 11 localities given in Table 4 using MABS and GB (four samples were rejected as explained in the caption to Fig. 7 and text). Closed squares represent samples that contain kyanite as the peak-*T* mineral, and open squares samples that contain sillimanite. Solid line is the K-S boundary.

TABLE 6. Average and 2σ values of *T* and *P* for Maine using GB and MABS.

Event	Zone	*n*	*T*(2σ)*	*P*(2σ)*
M3	Sil.-stau.	28	606(25)	4.67(86)
M3	Sil.-musc.	24	622(23)	4.32(71)
Hercynian	Sil.-musc.	6	641(8)	4.97(61)
Hercynian	Sil.-musc.-Ksp.	5	648(19)	5.91(150)

* 2σ is given in terms of the last one, two or three quoted figures

error for MABS is on the order of one kbar. For the *T* values, the errors are consistent with my estimate of ±15º relative and ±25º absolute, within the range of calibration. The MABS geobarometer needs more refinement and testing, but I believe that the present results show promise.

A final note

In using the thermochemical data that I and my coworkers have derived it is important to bear in mind that the data refer only to the system for which they were derived. At this time one must not attempt to add these numbers to thermodynamic databases. The reason for this is that the derived numbers tend to compensate for errors in other parts of the system being considered, especially in activity models and Margules models. This is the reason that the present approach does better on specific systems than databases. At some future time it might be possible to use the present results as constraints on databases, but only with careful attention to the errors involved.

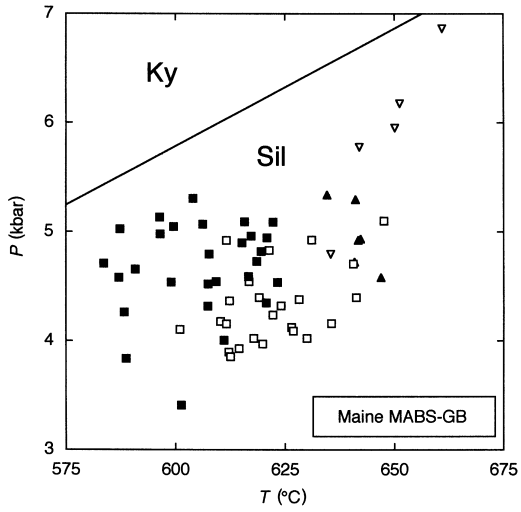

FIG. 9. Calculated *P* and *T* for all 63 sillimanite-bearing samples from Maine using MABS and GB. Squares represent M3, triangles represent Hercynian event. Closed squares = sillimanite-staurolite, open squares = sillimanite-muscovite, closed triangles = sillimanite-muscovite, open inverted triangles = sillimanite-muscovite-K-feldspar. The solid line is the K-S boundary.

References

Aranovich, L.Y., Lavrent'eva, I.V. and Kosyakova, N.A. (1988) Calibration of the biotite-garnet and biotite-orthopyroxene geothermometers corrected for the variable Al level in biotite. *Geochemistry International*, **25**, 50–59.

Berman, R.G. (1988) Internally-consistent thermodynamic data for stoichiometric minerals in the system Na_2O-K_2O-CaO-MgO-FeO-Fe_2O_3-Al_2O_3-SiO_2-TiO_2-H_2O-CO_2. *Journal of Petrology*, **29**, 633–645.

Berman, R.G. and Aranovich, L.Y. (1996) Optimized standard state and solution properties of minerals. I. Model calibration for olivine, orthopyroxene, cordierite, garnet, and ilmenite in the system FeO-MgO-CaO-Al_2O_3-TiO_2-SiO_2. *Contributions to Mineralogy and Petrology*, **126**, 1–24.

Dickerson, R.P. and Holdaway, M.J. (1989) Acadian metamorphism associated with the Lexington batholith, Bingham, Maine. *American Journal of Science*, **289**, 945–974.

Dutrow, B.L. and Holdaway, M.J. (1989) Experimental determination of the upper thermal stability of Fe-staurolite + quartz at medium pressures. *Journal of Petrology*, **30**, 229–248.

Dutrow, B.L., Holdaway, M.J. and Hinton, R.W. (1986) Lithium in staurolite: its petrologic significance. *Contributions to Mineralogy and Petrology*, **94**, 496–506.

Dyar, M.D. (1990) Mössbauer spectra of biotite from metapelites. *American Mineralogist*, **75**, 656–666.

Dyar, M.D., Perry, C.L., Rebbert, C.R., Dutrow, B.L., Holdaway, M.J. and Lang, H.M. (1991) Mössbauer spectroscopy of synthetic and naturally-occurring staurolites. *American Mineralogist*, **76**, 27–41.

Elkins, L.T. and Grove, T.L. (1990) Ternary feldspar experiments and thermodynamic models. *American Mineralogist*, **75**, 544–559.

Engi, M., Todd, C.S. and Schmatz, D.R. (1995) Tertiary metamorphic conditions in the eastern Lepontine Alps. *Schweizerische Mineralogische und Petrographische Mitteilungen*, **75**, 347–369.

Ferry, J.M. (1980) A comparative study of geothermometers and geobarometers in pelitic schists from south-central Maine. *American Mineralogist*, **65**, 720–732.

Ferry, J.M. and Spear, F.S. (1978) Experimental calibration of the partitioning of Fe and Mg between biotite and garnet. *Contributions to Mineralogy and Petrology*, **66**, 113–117.

Fletcher, C.J.N. and Greenwood, H.J. (1979) Metamorphism and structure of Penfold Creek area near Quesnal Lake, British Columbia. *Journal of Petrology*, **20**, 743–794.

Fuhrman, M.L. and Lindsley, D.H. (1988) Ternary-feldspar modeling and thermometry. *American Mineralogist*, **73**, 201–215.

Ganguly, J., Cheng, W. and Tirone, M. (1996) Thermodynamics of aluminosilicate garnet solid solution: new experimental data, an optimized model, and thermometric applications. *Contributions to Mineralogy and Petrology*, **126**, 137–151.

Gessmann, C.K., Spiering, B. and Raith, M. (1997) Experimental study of the Fe-Mg exchange between garnet and biotite: Constraints on the mixing behavior and analysis of the cation-exchange mechanisms. *American Mineralogist*, **82**, 1225–1240.

Guidotti, C.V. and Dyar, M.D. (1991) Ferric iron in metamorphic biotite and its petrologic and crystallochemical implications. *American Mineralogist*, **76**, 161–175.

Hawthorne, F.C., Ugaretti, I., Oberti, R., Caucia, F. and Callegari, A. (1993) The crystal chemistry of staurolite: I. Crystal structure and site occupancies. *The Canadian Mineralogist*, **31**, 551–582.

Hodges, K.V. and Spear, F.S. (1982) Geothermometry, geobarometry and the Al_2SiO_5 triple point at Mt. Moosilauke, New Hampshire. *American Mineralogist*, **67**, 1118–1134.

Holdaway, M.J. (2000) Application of new experimental and garnet Margules data to the garnet-biotite geothermometer. *American Mineralogist*, **85**, 881–892.

Holdaway, M.J. (2001) Recalibration of the GASP geobarometer in light of recent garnet and plagioclase activity models and versions of the garnet-biotite geothermometer. *American Mineralogist*, **86**, 1117–1129.

Holdaway, M.J. and Mukhopadhyay, B. (1995) Thermodynamic properties of stoichiometric staurolites $H_2Fe_4Al_{18}Si_8O_{48}$ and $H_6Fe_2Al_{18}Si_8O_{48}$. *American Mineralogist*, **80**, 520–533.

Holdaway, M.J., Guidotti, C.V., Novak, J.M. and Henry, W.E. (1982) Polymetamorphism and the isograd map for medium- to high-grade pelitic metamorphic rocks, west-central Maine. *Geological Society of American Bulletin*, **93**, 572–584.

Holdaway, M.J., Dutrow, B.L., Borthwick, J., Shore, P., Harmon, R.S. and Hinton, R.W. (1986*a*) Staurolite water content as determined by hydrogen extraction line and ion microprobe. *American Mineralogist*, **71**, 1135–1141.

Holdaway, M.J., Dutrow, B.L. and Shore, P. (1986*b*) A model for the crystal chemistry of staurolite. *American Mineralogist*, **71**, 1142–1159.

Holdaway, M.J., Dutrow, B.L. and Hinton, R.W. (1988) Devonian and Carboniferous metamorphism in west-central Maine: the muscovite-almandine geobarometer; the staurolite problem revisited. *American Mineralogist*, **73**, 20–47.

Holdaway, M.J., Mukhopadhyay, B., Dyar, M.D., Dutrow, B.L., Rumble, D., III, and Grambling, J.A. (1991) A new perspective on staurolite crystal chemistry: Use of stoichiometric and chemical end-members for a mole fraction model. *American Mineralogist*, **76**, 1910–1919.

Holdaway, M.J., Gunst, R.F., Mukhopadhyay, B. and Dyar, M.D. (1993) Staurolite end-member molar volumes determined from unit-cell measurements of natural specimens. *American Mineralogist*, **78**, 56–67.

Holdaway, M.J., Mukhopadhyay, B., Dyar, M.D., Guidotti, C.V. and Dutrow, B.L. (1997) Garnet-biotite geothermometry revised: New Margules parameters and a natural specimen data set from Maine. *American Mineralogist*, **82**, 582–595.

Lang, H.M. (1991) Quantitative interpretation of within-outcrop variation in metamorphic assemblages in staurolite-kyanite-grade metapelites, Baltimore, Maryland. *The Canadian Mineralogist*, **29**, 655–671.

Lang, H.M. and Rice, J.M. (1985*a*) Regression modeling of metamorphic reactions in metapelites, Snow Peak, northern Idaho. *Journal of Petrology*, **26**, 857–887.

Lang, H.M. and Rice, J.M. (1985*b*) Geothermometry, geobarometry and *T*-*X*(Fe-Mg) relations in metapelites, Snow Peak, northern Idaho. *Journal of Petrology*, **26**, 889–924.

McKenna, L.W. and Hodges, K.V. (1988) Accuracy versus precision in locating reaction boundaries:

Implications for the garnet-plagioclase-aluminum silicate-quartz geobarometer. *American Mineralogist*, **73**, 1205–1208.

McLellan, E. (1985) Metamorphic reactions in the kyanite and sillimanite zones of the Barrovian type area. *Journal of Petrology*, **26**, 789–818.

McMullin, D.W.A., Berman, R.G. and Greenwood, H.J. (1991) Calibration of the SGAM thermobarometer for pelitic rocks using data from phase equilibrium experiments and natural assemblages. *The Canadian Mineralogist*, **29**, 889–908.

Mukhopadhyay, B., Sabyasachi, B. and Holdaway, M. J. (1993) A review of Margules-type formulations for multicomponent solutions with a generalized approach. *Geochimica et Cosmochimica Acta*, **57**, 277–283.

Mukhopadhyay, B., Holdaway, M.J. and Koziol, A.M. (1997) A statistical model of thermodynamic mixing properties of Ca-Mg-Fe^{2+} garnets. *American Mineralogist*, **82**, 165–181.

Novak, J.M. and Holdaway, M.J. (1981) Metamorphic petrology, mineral equilibria, and polymetamorphism in the Augusta Quadrangle, south-central Maine. *American Mineralogist*, **66**, 51–69.

Perchuk, L.L. and Lavrent'eva (1983) Experimental investigation of exchange equilibria in the system cordierite-garnet-biotite. Pp. 199–239 in: *Kinetics and Equilibrium in Mineral Reactions* (S.K. Saxena, editor). Advances in Physical Geochemistry, **3**, Springer, New York.

Pigage, L.C. (1976) Metamorphism of the Settler Schist, southwest of Yale, British Columbia. *Canadian Journal of Earth Science*, **13**, 405–421.

Pigage, L.C. (1982) Linear regression analysis of sillimanite-forming reactions at Azure Lake, British Columbia. *The Canadian Mineralogist*, **20**, 349–378.

Spear, F.S., Kohn, M.J. and Paetzold, S. (1995) Petrology of the regional sillimanite zone, west-central New Hampshire, U.S.A., with implications for the development of inverted isograds. *American Mineralogist*, **80**, 361–376.

Todd, C.S. and Engi, M. (1997) Metamorphic field gradients in the Central Alps. *Journal of Metamorphic Geology*, **15**, 513–530.

Tracy, R.J. (1975) *High grade metamorphic reactions and partial melting in pelitic schist, Quabbin Reservoir area, Massachusetts*. PhD thesis, University of Massachusetts, Amherst, Massachusetts, USA, 127 pp.

[*Manuscript received 22 July 2003: revised 5 January 2004*]